National Weather Service
Office of Meteorology

Technical Procedures Bulletin

Series No. **412**

Program Requirements and Development Division, Silver Spring, MD 20910

FIRST BULLETIN ON THIS SUBJECT

This Technical Procedures Bulletin (TPB), written by Thomas Black, Dennis Deaven and Geoffrey DiMego of the Development Division, National Meteorological Center, describes the 80-km version of the new Eta model.

The Eta Model differs from current operational models in structure, numerics, and physical parameterizations with the aim of producing an overall improvement in forecast skill, particularly in quantitative precipitation. Because of its early data cutoff and its 80-km resolution, this initial implementation will be known as the 'Early' or 80-km version of the Eta model. Future versions will be at mesoscale resolution and will run later in the production schedule. The planned implementation date for the 80-km Eta model is June 8, 1993, at 1200 UTC.

Operational users of the Eta model and its associated products may be particularly interested in Section 4, entitled "Objective Verification Results". It includes results of the objective verification of the Eta model, which occurred in March 1993.

Mary M. Glackin
Chief, Services Development Branch

U.S. DEPARTMENT OF COMMERCE   National Oceanic and Atmospheric Administration
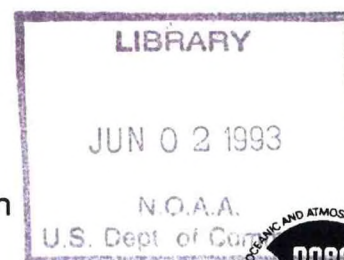
The Step-Mountain Eta Coordinate Model: 80 km 'Early' Version and Objective Verifications

by Thomas Black, Dennis Deaven and Geoffrey DiMego,
Development Division, National Meteorological Center

1. INTRODUCTION

Development of a new numerical weather prediction model is continuing with its ultimate goal being to provide accurate mesoscale forecasts in the mid-1990s and beyond. One of the immediate goals, however, is to provide an improved early look at the synoptic-scale forecast in place of that provided by the Limited-area Fine-mesh Model (LFM) which will be phased out for the contiguous United States, beginning in June 1993 (the LFM will be continue to be run in support of Alaska Region operations until mid-1994). The new model, called the Eta Model (Black, 1988; Mesinger et al.,1988; Janjic, 1990), differs from current operational models in structure, numerics, and physical parameterizations (see Table 1) with the aim of producing an overall improvement in forecast skill, particularly in quantitative precipitation (Mesinger et al., 1990). Because of its early data cutoff and its 80-km resolution, this initial implementation will be known as the 'Early' or 80-km version of the Eta model. Future versions will be at mesoscale resolution and will run later in the production schedule.

A brief description of some of the primary aspects of the model follows in Section 2. Section 3 deals with the Eta-based analysis and Section 4 presents results of objective verification of the Eta model versus the LFM during the spring of 1993.

2. THE ETA MODEL

2.1 The Eta Coordinate and Step-Mountains

This model has acquired the name of its vertical coordinate, the Greek letter - eta. The eta coordinate system (Mesinger, 1984) is actually only a simple variation of the commonly used sigma coordinate system employed at the National Meteorological Center (NMC) in the LFM, the Nested Grid Model (NGM) and the global spectral model. Both coordinate systems are normalized and pressure-based. However, while the sigma coordinate varies from 0 to 1 between the top of the model domain and the model's ground surface, the eta coordinate varies from 0 to 1 between the top of the model's vertical domain (currently 50 mb) and mean sea-level. In other words, eta is normalized with respect to the mean sea-level pressure whereas sigma is normalized with respect to the surface pressure. Both systems' coordinate surfaces are thus fairly horizontal over the ocean and over flat terrain. However, in regions where the ground elevation changes rapidly, the horizontal variation of sea-level pressure is much less than that of surface pressure. The result is that the sigma surfaces must slope steeply just as the ground does. The lack of slope on the eta coordinate surfaces can produce a significant numerical benefit when computing the pressure-gradient force near steeply sloping terrain (Mesinger and Black, 1992). Given this horizontal nature of eta, it seems natural to render the model's topography into the shape of steps - hence the term step-mountain. Figure 1 shows a vertical cross-section through the lowest layers of a hypothetical Eta model.

2.2 The Horizontal Domain

The horizontal domain of the Eta model and the actual mass variable grid-point locations are shown in Figure 2a. The grid used in the Eta model is semi-staggered, which means that the wind components are predicted on alternate points to those of all the mass variables (such as temperature, specific humidity, and surface pressure). This is seen in Figure 1 by the alternating u and T symbols in each model layer, where u represents both horizontal wind com-

ponents and T represents all mass variables other than surface pressure. The circled u's (as well as the v's in the same places) on the sides of the steps are assigned a value of zero.

The horizontal resolution is approximately 80 km in the 'Early' version of the Eta model. This means that the distance between a mass point and its nearest mass point neighbor is about 80 km. Each row (column) lies along a parallel (meridian) of the model's rotated latitude (longitude). In other words, the grid is oriented just as if the earth's latitude/longitude lines were rotated by taking the point where the equator crosses the prime meridian and shifting it to the center of the region over which the model is making its forecasts. The grid's central point, currently located at 52°N and 111°W, is at the intersection of the rotated equator and the rotated prime meridian. The effect of positioning the "new" equator across the center of the forecast domain is simply to minimize the convergence of meridians. It has the numerically advantageous effect of minimizing the difference in Δx and Δy across the grid. For the sake of comparison, Figure 2b shows the LFM grid points on the same polar-stereographic background as is used for the Eta model mass-variable points in Figure 2a. Because the LFM's grid is polar stereographic, its grid points create a regular mesh on this projection, whereas the Eta model's rotated latitude/longitude grid, Figure 2a, does not.

2.3 The Vertical Domain

There are 38 layers in this version of the Eta model. The lowest layer over the ocean is defined to be exactly 20 meters thick for the standard atmosphere. The layers thicken gradually with height into the mid-troposphere then thin again (with respect to mass) as the upper part of the domain is reached. A secondary maximum in resolution was placed at around 250 mb in order to capture more details in the vertical structure of the jet stream.

Figure 3 depicts the relative thickness of all 38 model layers. Each step of the model's topography is centered on a mass point and has a velocity point over each vertex. The top of each step coincides exactly with one of the interfaces between the model's layers. The algorithm used to create the steps tends to maximize their heights based upon the detailed surface elevation data (so-called silhouette topography; Mesinger and Collins, 1987).

2.4 The Forecast

The split-explicit approach is used in the integration of the model equations. This means that each process (advection, convection, etc.) is computed sequentially, whereupon each of the primary prognostic variables is updated to reflect the influence of the particular process. The fundamental time step of this version of the Eta model is that of the adjustment of the mass and momentum fields, caused by the pressure gradient and Coriolis forces, and is equal to 200 seconds. The time steps of other processes are integral multiples of this fundamental one. Specifically, the time step of advective processes is twice that of the adjustment, while the time step of most physical processes, such as convection and turbulence, is four times that of the adjustment.

3. THE ETA-BASED ANALYSIS

Initial conditions for the 80-km Eta model are provided by an analysis scheme based upon optimum interpolation. The computer program, coding techniques and algorithms are very similar to those used by the current regional analysis system (DiMego, 1988). The analysis is cast upon a regular latitude-longitude grid in the horizontal and the eta coordinate in the vertical. The horizontal resolution is fixed at 0.75 degrees in both the north-south and west-east directions, with 295 points contained in the west-east direction and 120 points in the north-south direction. This grid is large enough to superscribe the actual model domain shown in Figure 2a. In the vertical, analysis is performed in the model coordinate at the 38 layers distributed in the eta coordinate from the surface to 50 mb, as depicted in Figure 3.

The first guess is provided by the Global Data Assimilation System (GDAS) in the form of T-126 resolution, sigma-coordinate, spectral

coefficients of the global spectral model (Kanamitsu, 1989). The transformed spectral coefficients are cast onto the 295 x 120 analysis grid horizontally and interpolated vertically from the sigma coordinate of the global spectral model to the 38 layers of the Eta model. Observational increments are obtained by differencing the observations and the first guess at each of the observation locations. Sounding data (heights and winds) are treated at a vertical resolution of every 25 mb. Wind profiler and domestic aircraft (ACARS) reports represent an important and plentiful source of wind data. All available surface land and marine reports are fully utilized in the analysis. The data cutoff remains nominally one hour and 15 minutes after observation time.

The optimum interpolation weights are calculated at each grid point by using the nearest 30 observation locations. The analysis is multivariate, such that height increments affect the wind analysis and wind increments affect the height analysis. The 30 weighted-observation increments are summed to form an analysis increment at each grid point, that is combined with the first guess values to form the full-field analysis. The initial conditions for the Eta model are obtained by interpolating these fields from the analysis grid to the model grid. Although the same vertical coordinate is used in the analysis and forecast model, the interpolation from the analysis grid to the model grid must be performed in three-dimensional space to account for the different specifications of the step orography. Future versions of the Eta-based analysis system will utilize the same horizontal grid specification for both the analysis and the forecast model, allowing the direct application of analysis increments to the first guess.

4. OBJECTIVE VERIFICATION RESULTS

This section will deal with the performance of the Early Eta model as compared to the LFM, using several objective scores employed regularly by the Regional and Mesoscale Modeling Branch of the Development Division of NMC. Generally, the period covered is the month of March 1993. The Meteorological Operations Division (MOD) of NMC subjectively

evaluated the performance characteristics of the Eta model versus the LFM during this same period. Their results will be presented in a subsequent TPB.

4.1 Grid-to-Grid Verifications

The Eta model and LFM forecasts in grid-point form have been verified against selected 'observed' fields, also in grid-point form. All model and verification fields are on (or are put on via interpolation) the 80-km polar-stereographic grid of the innermost grid of the NGM -- the so-called C-grid. Verifications were performed for only the North American land points of this grid, and summed quantities were weighted by the inverse map-scale factor (proportional to area). The Regional Analysis and Forecast System (RAFS) (DiMego, et al. 1992) analysis fields on the C-grid are used throughout this section as the verification.

4.1.1 Anomaly Correlation

Figure 4 shows the results for anomaly correlation coefficient for height at four pressure levels: 1000, 700, 500 and 200 mb. This score is the correlation between the forecast departure and the observed departure from climatology for a given day. A perfect forecast would reproduce the observed anomaly (analysis minus climatology) and would have a correlation of 1. The RAFS analyses were used in computing the observed anomaly. For the month of March 1993, all scores were quite high - note the y-axis scale of Figure 4. The Eta model has a consistent, albeit slight, edge over the LFM at all ranges and at each of the four levels. The maximum difference is 0.018 at 48 hr at 700 mb.

4.1.2 Four Scores: Relative Humidity and Lifted Index

Four scores routinely used in our grid-to-grid verification package were computed after the evaluation period. These four scores are used in the figures discussed in this section. The first score is based on the S1 score (Teweles and Wobus, 1954; Hirano, 1992). This score verifies forecast gradients of a field against

the observed gradients of the field. S1 is expressed as:

$$S1 = 100\% \times \frac{|ERR|}{|GRAD|}, \quad \text{where}$$

$|ERR|$ is the sum of the magnitudes of the forecast error in the gradient component in each direction and $|GRAD|$ is the sum of the magnitudes of either the forecast or observed gradient component, whichever is larger. Gradient components and their error are calculated in both Cartesian directions within the 80-km polar-stereographic grid. Although normally expressed in percent (%), we choose to express the S1 score as:

$$S1 = 1.0 - \frac{|ERR|}{|GRAD|}.$$

S1 will then have a similar range (1.0 to 0.0) and interpretation (1.0 being a perfect forecast) as a correlation coefficient.

The second score used is the field correlation coefficient which is the correlation of the forecast with the verifying analysis. The third score used is the tendency correlation coefficient, which correlates the 12-hour forecast change with the observed change. The fourth score used is the tendency S1 score, which verifies gradients in the 12-hour change field. All scores use the RAFS analysis (on the 80-km grid) as verification. For all four scores, a perfect forecast would achieve a score of 1; therefore, a bigger score is better.

Figures 5 and 6 show grid-to-grid results for the four scores for the field of relative humidity at 850 and 700 mb, respectively. Although the S1 scores are generally at a lower level than the correlation coefficients, the scores for relative humidity are quite small, indicating the difficulty of predicting the moisture gradients. The Eta model does produce higher scores (better forecasts) at both levels, for all four scores and at each of the forecast ranges.

Figure 7 shows results for the four scores for grid-point fields of lifted index. This is the surface-to-500 mb lifted index, which is common to the output of the Eta, LFM and RAFS. Other lifted indices are produced from the Eta model (Treadon, 1993) and NGM but have no analogous field from the LFM. Steven Weiss of the National Severe Storms Forecast Center (NSSFC) has indicated (personal communication) that the RAFS initial fields of lifted index are in reasonably good agreement with observed values from rawinsonde data, justifying their use here as verification. The results shown in Figure 7 indicate the Eta model verifies better than the LFM for all scores and all ranges (except at 48 hr in the S1 score), but by fairly modest amounts.

4.1.3 Four Scores: Height, Temperature, Vorticity and Wind Speed

The four scores used above for relative humidity and lifted index have also been used to verify the fields of height, temperature, vorticity of the wind field, and the velocity of the wind field at each of the lowest eight mandatory pressure levels. This represents 32 times more information than is presented in Figures 5, 6 or 7 (four variables at eight levels). Rather than subject the reader to such an overload of figures, we have produced summary displays of the differences between the Eta model scores and the LFM scores. The summaries for height and temperature are depicted in Figure 8a and for the vorticity of the wind and the wind speed in Figure 8b. Results are presented for the four scores (in the order listed below each figure) at the indicated pressure levels. Thus, there are 64 comparisons per level, or 256 comparisons per figure, for a total of 512.

Positive values of this difference imply a higher score or correlation coefficient for the Eta than the LFM. Figures 8a and 8b demonstrate that the Eta model scores higher (better) than the LFM in the vast majority of comparisons and, for those very few comparisons which are negative, their magnitude is small.

4.2 Verification versus Rawinsonde Observations

Eta model and LFM forecasts have been verified against North American rawinsonde observations (RAOBs). This includes all RAOBs of any type that reported during the 35-day period from February 26 to April 1, 1993, anywhere within the 80-km domain. A simple bi-linear interpolation is used to obtain a forecast value at the observation location using model fields on mandatory pressure levels. A quality-control step for the observations uses the RAFS analysis. Bias, the average of all differences (forecast minus observation) in the domain for the 35-days, and standard deviation about this mean are shown.

4.2.1 Specific Humidity

The results of comparisons with RAOB specific humidity data are shown in Figure 9 for the bias and in Figure 10 for the standard deviation for the six lowest mandatory pressure levels. The Eta model tends to be too moist (positive) at the 1000-mb level, but to a degree that is not as severe as the LFM is too dry (negative). A slight tendency for the Eta model to be too dry is demonstrated at the 500-mb and 400-mb levels, but the trend is for this tendency to decrease with forecast range. The standard deviations for the Eta model are less (better) than the LFM at the lowest three levels, becoming essentially the same at the upper three levels.

4.2.2 Height

Figure 11 shows the bias statistics for the height of nine pressure surfaces from 1000 mb to 150 mb. Both models clearly forecast the heights to be too low (negative bias), and the trend is for increasing values with forecast range, especially for the LFM at upper levels. Compared to the LFM, at the lowest three levels, the Eta model has much less bias, whereas, in the middle three levels it has a greater bias. This is evidence of, and a consequence of, a cold bias in the middle troposphere in the Eta. The 1000-500 mb thickness bias in the Eta model can be inferred by differencing the bias values. This process yields values ranging from just under 10 m too low at 12 hours into the forecast

to a value near 20 m at the 48-hour range. The comparison of standard deviations for height are shown in Figure 12. The advantage of the Eta model over the LFM is evident at all levels and at all ranges of the forecast.

4.2.3 Temperature

The bias statistics for temperature are shown in Figure 13. Not surprisingly, the cold bias in the Eta model is evident at 700 mb and 500 mb, and to a lesser extent, at 850 mb. Near jet level, 300 mb, 250 mb and 200 mb, there is a slight warm bias of less than 0.5°C which decreases with forecast range. At the uppermost levels, the growth of a strong cold bias in the LFM is not as evident in the Eta. The 1000-mb warm bias, which reaches 2°C by 48 hours, is being investigated. It is restricted to relatively few reports at this level.

Standard deviation statistics for temperature are presented in Figure 14. Except at 1000 mb, the Eta model results are as good as, or better than, the LFM at all levels and at all ranges. At the levels which surround the tropopause (300 mb, 250 mb and 200 mb), the Eta is clearly superior. This is due to the Eta's higher vertical resolution compared to the LFM's - despite the fact that the LFM has the tropopause as a coordinate surface.

4.2.4 Wind

Figure 15 presents the bias statistics for the wind speed and Figure 16 the root-mean-square (RMS) vector wind statistics. It is clear that for both wind statistics, the Eta model is markedly superior. The wind speed bias in the Eta model never exceeds 1 m/s, except (just barely) at 48 hours at 300 mb and 250 mb. The LFM, on the other hand, has a bias in excess of this at all levels except 200 mb, already by the 12-hour point of its forecast. The Eta model winds at low-levels tend to be too strong, indicating circulations that are a little too vigorous. Whereas the bias is computed from the speed alone, the RMS vector error is calculated from the error in both wind components. The RMS wind vector errors are quite low for the Eta model and, compared to the LFM, represent

an impressive degree of improvement. The level of error at 48 hours into the Eta forecast has barely reached that of the LFM at 12 hours - a full day and a half advantage.

4.3 Precipitation Verification

Objective verification of precipitation amounts by the Development Division has been greatly improved with the use of the Office of Hydrology's River Forecast Centers database. This contains reports from as many as ten thousand locations covering the lower 48 United States. A "box average" analysis of the 24-hour (1200 UTC to 1200 UTC) amounts is performed on the 80-km Eta model grid after a four-day delay, to allow for late arriving reports to enter the database. Verification is performed on a 1001-point subset of the Eta grid including only United States points where the grid-box contains at least one reporting station. The station density was determined by collecting all stations that reported during the period June 1991 through February 1992. A depiction of the station density for this period is contained in Figure 17, and the portion of the 80-km Eta model grid used for verification is presented in Figure 18.

The LFM precipitation amounts are distributed to the 80-km grid assuming uniform precipitation intensity across the grid square and in a manner which preserves the total area-integrated amount. An Equitable Threat Score (ETS) is computed as well as the bias:

$$ETS = \frac{H - CH}{F + O - H - CH} \quad \text{and} \quad BIAS = \frac{F}{O}, \quad \text{where}$$

F is the number of forecast points above a threshold, O is the number of observed points above a threshold, H is the number of hits above a threshold, and CH is the expected number of hits in a random forecast of F points for O observed points, which is equal to:

$$CH = \frac{F \times O}{1001}, \quad \text{where}$$

the denominator is the number of points in the verification domain. The ETS, through the use of CH, attempts to negate the reward achieved in a normal threat score by increasing hits via increasing the bias. It has a similar range and interpretation as the normal threat score.

Figure 19 presents the results of the ETS calculations. These results are for March 1993, and include the 00-24 and 24-48 hour periods from 1200 UTC runs and the 12-36 hour period from 0000 UTC runs. The rain/no-rain category (0.01") is won by the LFM, but the Eta does better than the LFM in the 0.10", 0.25" and 0.5" thresholds and equally well at 0.75" and 1.0". While the LFM scores better at the highest thresholds (1.5" and 2.0"), its exceedingly high bias depicted in Figure 20 at these thresholds renders the LFM's victory there somewhat questionable. Figure 21 and 22 show results for the first 24 days of April 1993, during which the Eta model has nearly tied the LFM at the rain/no-rain threshold and wins decisively all of the remaining categories.

To provide a broader perspective, the precipitation results for the summer months of 1992 are presented in Figure 23 for the equitable threat score and for the bias in Figure 24. These results are for the 17-layer version of the Eta model being run at that time, but are considered representative of the model's capability during the warm season. The Eta model, in fact, has a markedly superior capability compared to the LFM at all thresholds. The LFM continues to have bias problems during the summer, but now it produces much too little precipitation. The Eta model, on the other hand, has very little bias, with values uniformly near 1.0 across all thresholds, which is a desirable behavior similar to its performance during Spring 1993.

5. SUMMARY

A brief description of the Eta model and its analysis have been provided along with results from a battery of objective verification scores. Grid-to-grid comparisons between the Eta and the LFM for March 1993 using the RAFS analysis for verification were performed for correlation coefficient, S1 score, 12-hour tendency and

tendency S1 for the parameters of lifted index, relative humidity, height, temperature, wind speed and vorticity. In an overwhelming majority of cases, the Eta model scored higher than the LFM. Forecast-to-RAOB verifications were computed at the mandatory levels for a 35-day period in Spring 1993. Bias statistics, while generally favoring the Eta over the LFM, also indicated the following: 1000-mb Eta forecasts were too wet (0.5 g/kg) and too warm (1.5 - 2.0°C); low-level wind speeds were too strong; mid-level heights were too low as a result of temperatures being too cold in the lower troposphere. Jet-stream wind speeds were too low, as usual, but only half as much as the LFM. Standard deviation results for specific humidity, height, temperature and wind were universally favorable to the Eta model. RMS vector-wind errors at 48 hours in the Eta were at the same level as the 12-hour errors in the LFM - a full day and a half advantage at all levels. Verification of 24-hour precipitation amounts showed a clear advantage for the Eta model during the warm seasons. Cold season (March 1993) performance favored the LFM in only the rain/no-rain category - since extremely high biases at the larger amounts were present in the LFM statistics. Overall, the Eta model has little or no bias in either warm or cold seasons.

6. REFERENCES

Betts, A. K., 1986: A new convective adjustment scheme. Part I: Observational and theoretical basis. *Quart. J. Roy. Meteor. Soc.*, **111**, 1306-1335.

___, and M. J. Miller, 1986: A new convective adjustment scheme. Part II: Single column tests using GATE wave, BOMEX, ATEX and Arctic air-mass data sets. *Quart. J. Roy. Meteor. Soc.*, **112**, 693-709.

Black, T. L., 1988: The step mountain, eta coordinate model: A documentation. NWS/NMC Development Division Paper, 47 pp [Available from NMC, 5200 Auth Road, Washington, D. C. 20233].

DiMego, G., 1988: The NMC regional analysis system. *Mon. Wea. Rev.*, **116**, 977-1000.

___, K. E. Mitchell, R. A. Petersen, J. E. Hoke, J. P. Gerrity, J. J. Tuccillo, R. L. Wobus and H.-M. H. Juang, 1992: Changes to NMC's Regional Analysis and Forecast System. *Wea. Forecasting*, **116**, 977-1000.

Fels, S. B. and M. D. Schwarztkopf, 1975: The simplified exchange approximation: A new method for radiative transfer calculations. *J. Atmos. Sci.*, **32**, 1475-1488.

Hirano, R., 1992: The NMC's historical 36- (30-) hour S1 score record. NMC Office Note 389, NWS/NMC, 29 pp [Available from NMC, 200 Auth Road, Washington, D.C. 20233].

Kanamitsu, M., 1989: Description of the NMC Global Data Assimilation and Forecast System. *Wea. Forecasting*, **4**, 335-342.

Janjic, Z. I., 1990: The step-mountain coordinate: Physical package. *Mon. Wea. Rev.*, **118**, 1429-1443.

Mellor, G. L. and T. Yamada, 1982: Development of a closure model for geophysical fluid systems. *Rev. Geophys. Space Phys.*, **20**, 851-875.

Mesinger, F., 1984: A blocking technique for representation of mountains in atmospheric models. *Riv. Meteor. Aeronautica*, **44**, 195-202.

___, and W. G. Collins, 1987: Review of the representation of mountains in numerical weather prediction models. Observation, Theory and Modeling of Orographic Effects, Seminar Notes Vol. 2. ECMWF, Reading, UK, 1-28.

___, Z. I. Janjic, S. Nickovic, D. Gavrilov and D. Deaven, 1988: The step-mountain coordinate model description and performance for cases of Alpine lee cyclogenesis and for a case of Appalachian redevelopment. *Mon. Wea. Rev.*, **116**, 1493-1518.

___, T. Black, D. W. Plummer and J. H. Ward, 1990: Eta model precipitation forecasts for a period including Tropical Storm Allison. *Wea. Forecasting*, **5**, 483-493.

___, and ___, 1992: On the impact on forecast accuracy of the step-mountain (Eta) vs. sigma coordinate. *Meteor. Atmos. Phys.*, **50**, 47-60.

Teweles, S., and H. Wobus, 1954: Verification of prognostic charts. *Bull. Amer. Meteor. Soc.*, **35**, 455-463.

Treadon, R., 1993: Enhanced output capabilities of the Eta model. NMC Office Note, in preparation [Available from NMC, 5200 Auth Road, Washington, D. C. 20233].

Characteristic \ Model	LFM	Eta
Grid type	Unstaggered Arakawa A	Semi-staggered Arakawa E
Fundamental prognostic variables	Potential Temperature, u, v, thickness (sfc & tropopause pressure), precipitable water	Temperature, u, v, surface pressure, specific humidity, turbulent kinetic energy
Horizontal resolution	polar-stereographic 190.5 km at 60°N	14/26° rotated latitude 15/26° rotated longitude approximately 80 km
Vertical resolution	7 sigma layers	38 eta layers
Time differencing	Leapfrog	Split-explicit: Adjustment uses forward-backward scheme, Horiz. advection uses a modified Euler-backward, Vertical advection uses Euler-backward
Physics	Moist convective adjustment Grid-scale rain No vertical eddy transport Bulk sfc fluxes simple radiation – one degree cooling per day	Betts(1986)/Betts-Miller (1986) convection Grid-scale rain Mellor-Yamada (1982) Level 2.5 Mellor-Yamada(1982) L 2 Fels-Schwarztkopf (1975) radiation scheme
Analysis	Successive-corrections 10 isobaric levels	Optimum-interpolation 38 eta layers
Initial balancing	Removal of initial divergence	None
Boundary conditions	One-way interaction from AVN forecast of preceding cycle	One-way interaction from AVN forecast of preceding cycle

Table 1. Basic characteristics of the LFM and the Early Eta model.
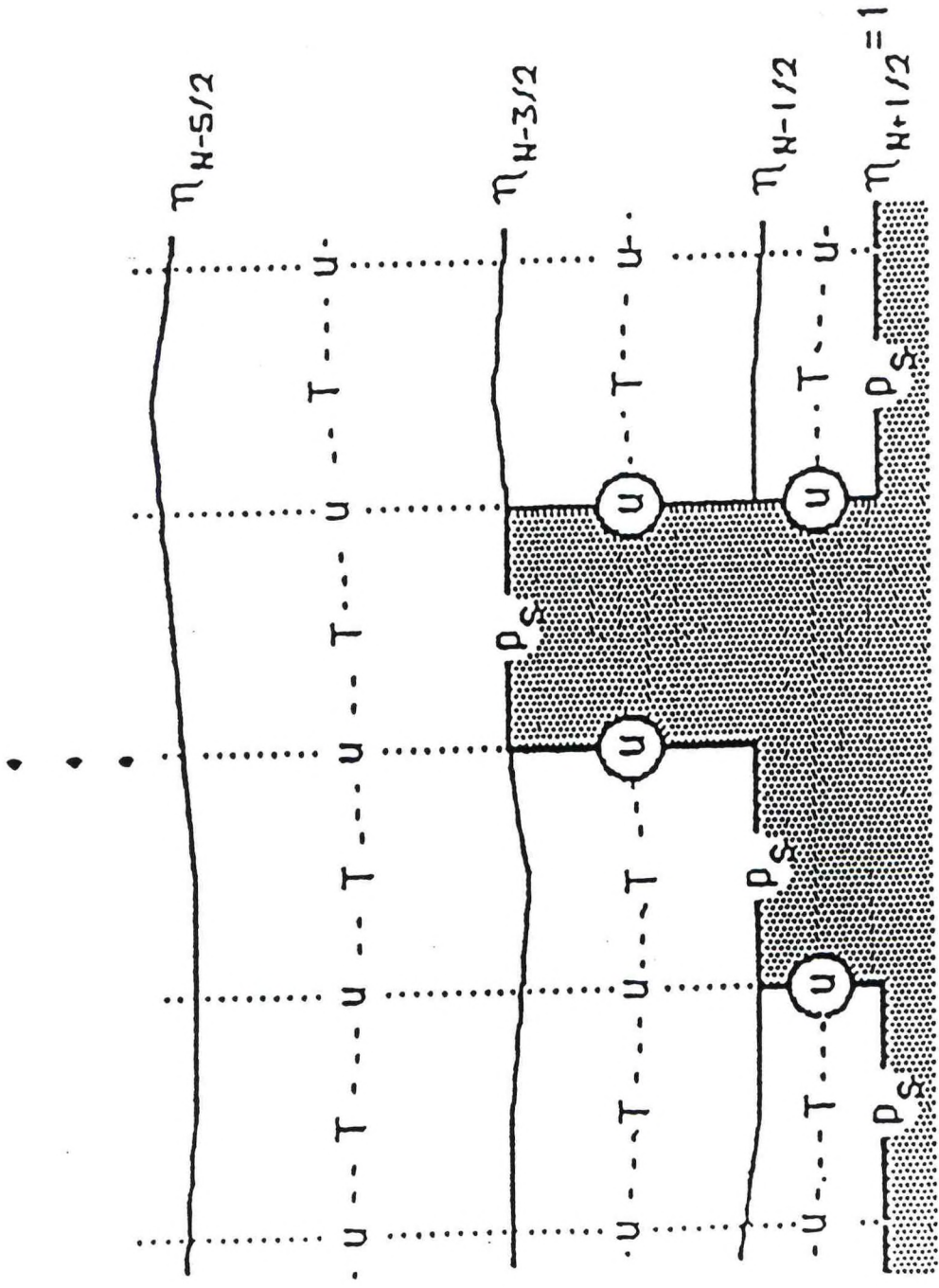
Figure 1. Schematic of a vertical cross-section of the lowest layers of an Eta coordinate model. In this figure, T represents all mass variables (e.g. temperature and specific humidity) and u represents both horizontal components of the wind. The quantity P_s is the surface pressure. The circled u's on the sides of the steps indicate wind points which are defined as zero.

TPB 412

80 KM ETA DOMAIN (92 X 141)
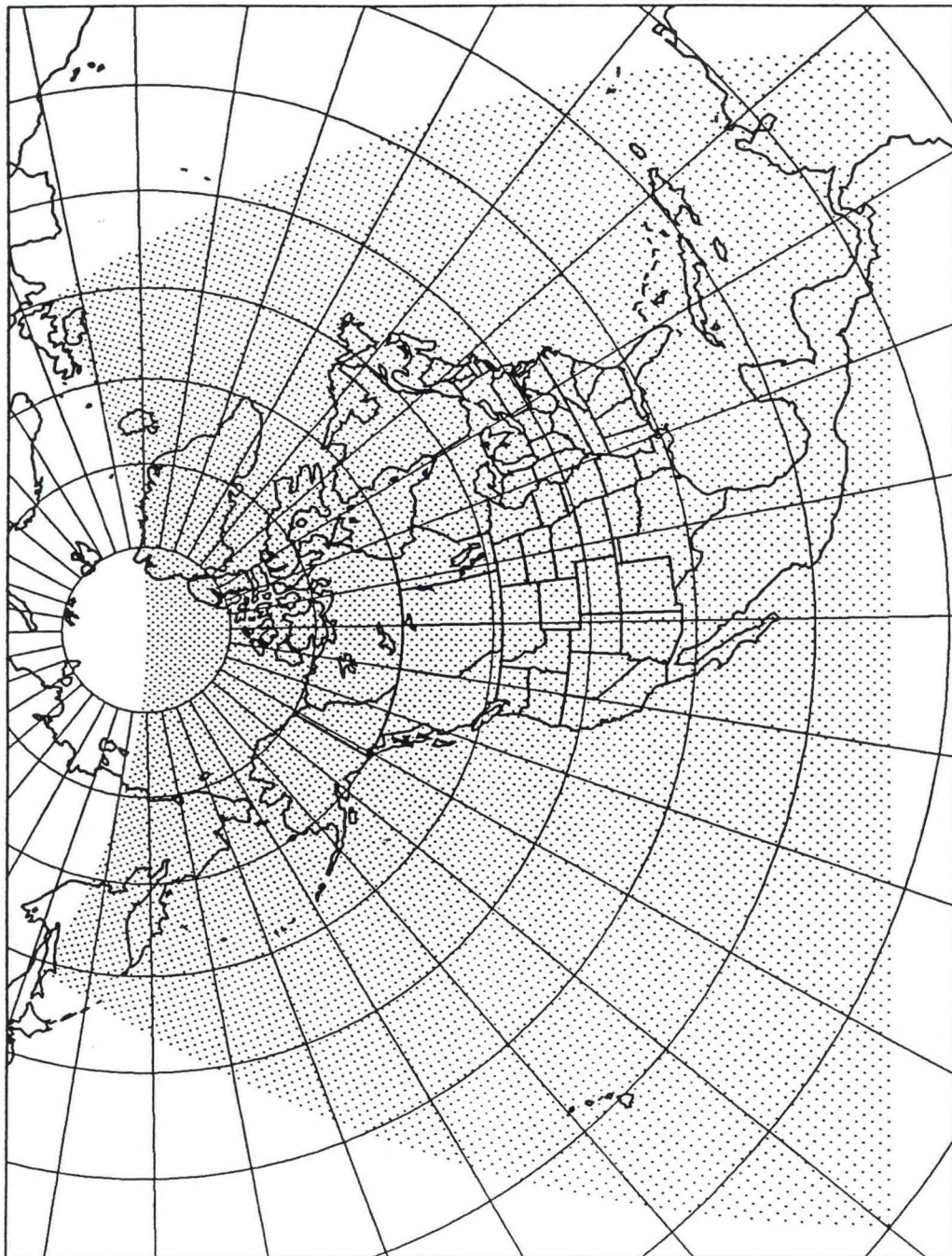
Figure 2a. The horizontal area (and grid points) covered by the 80-km Early Eta model forecasts.

190.5 KM LFM DOMAIN (53 BY 45)
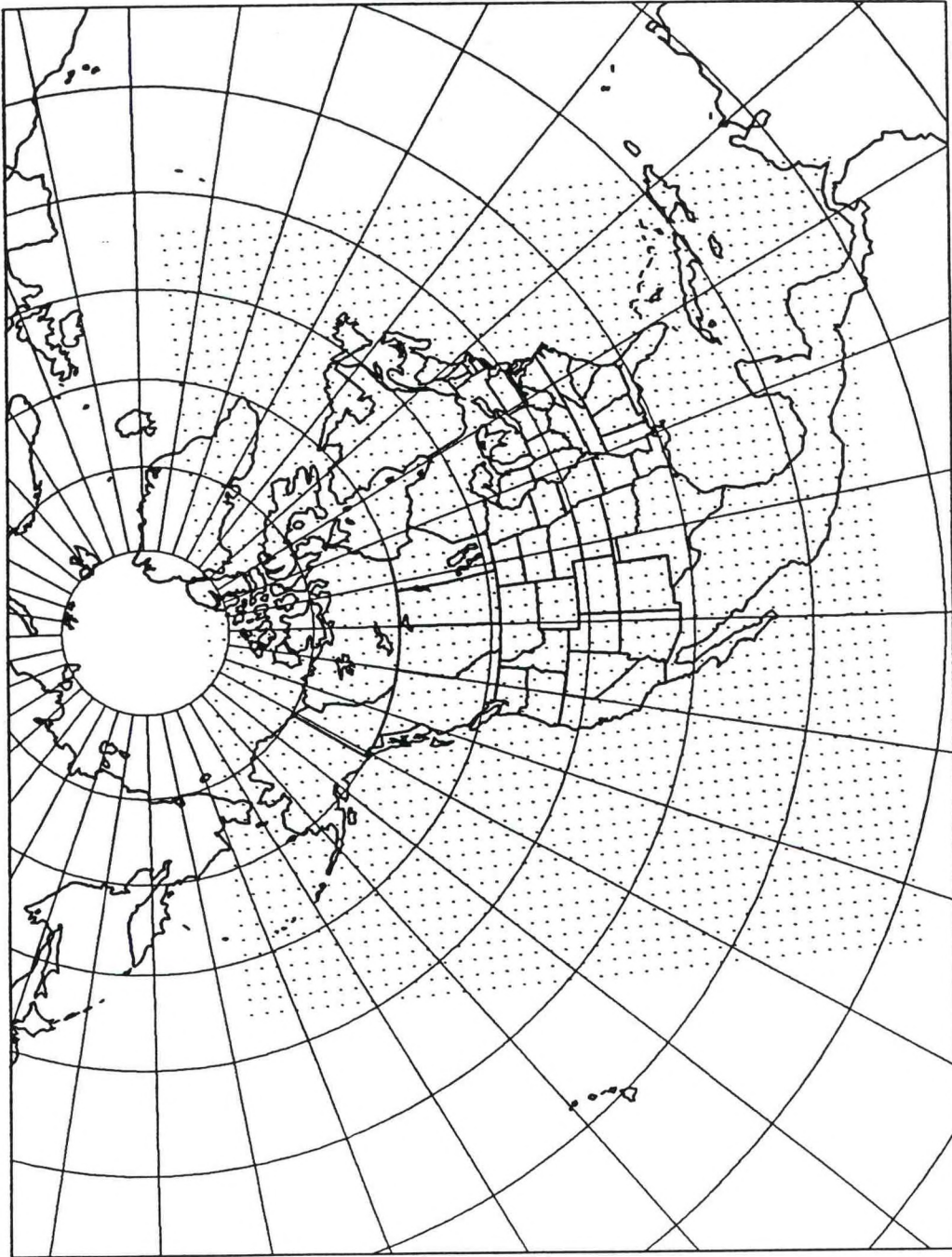
Figure 2b. The horizontal area (and grid points) covered by the 190.5-km LFM.
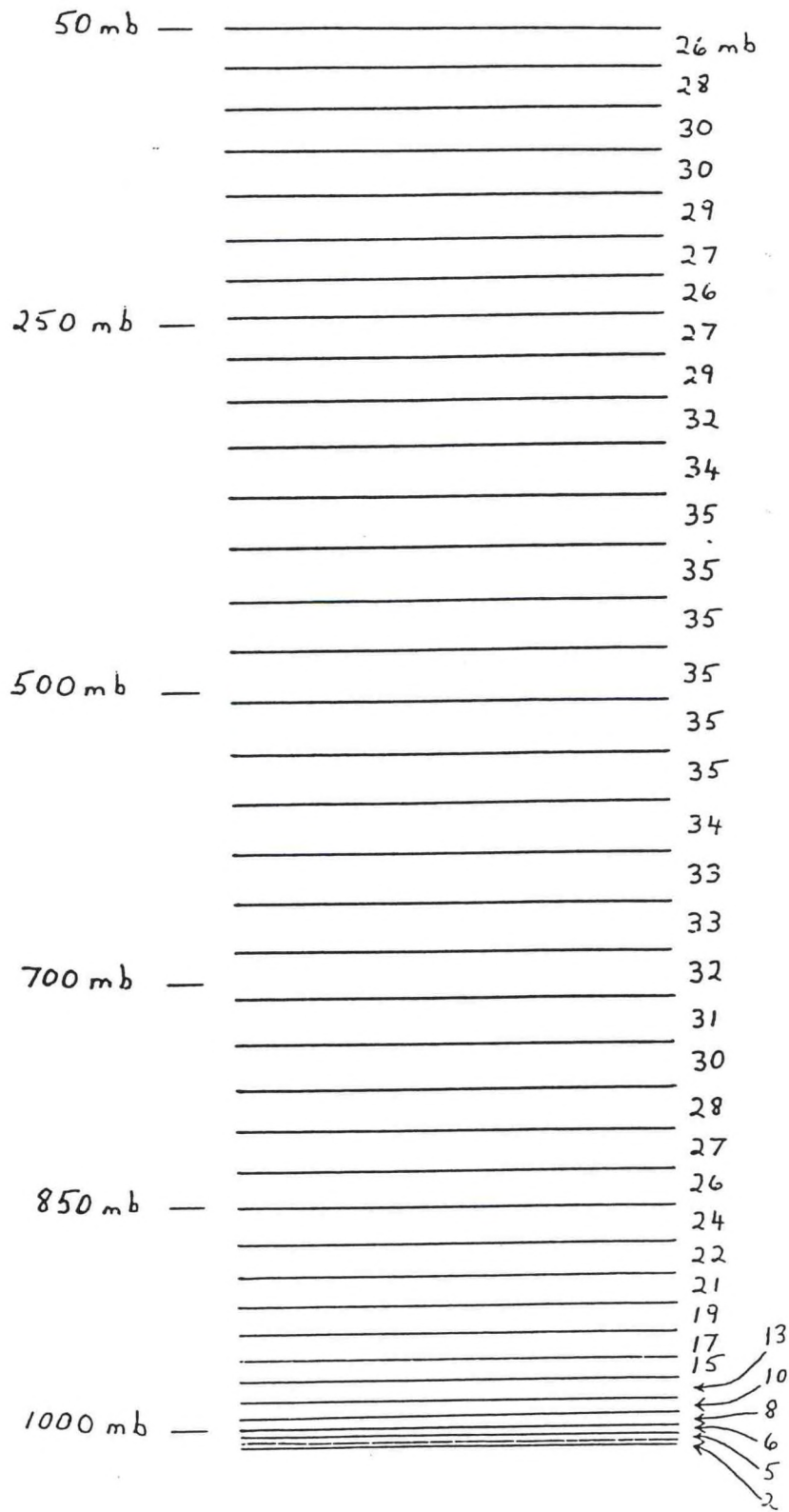
Figure 3. The 38 layers of the Early Eta model, drawn proportional to their thickness in mass (mb) for the standard atmosphere.

Anomaly Correlation Coefficient Height
North America 3/2/93 - 3/31/93
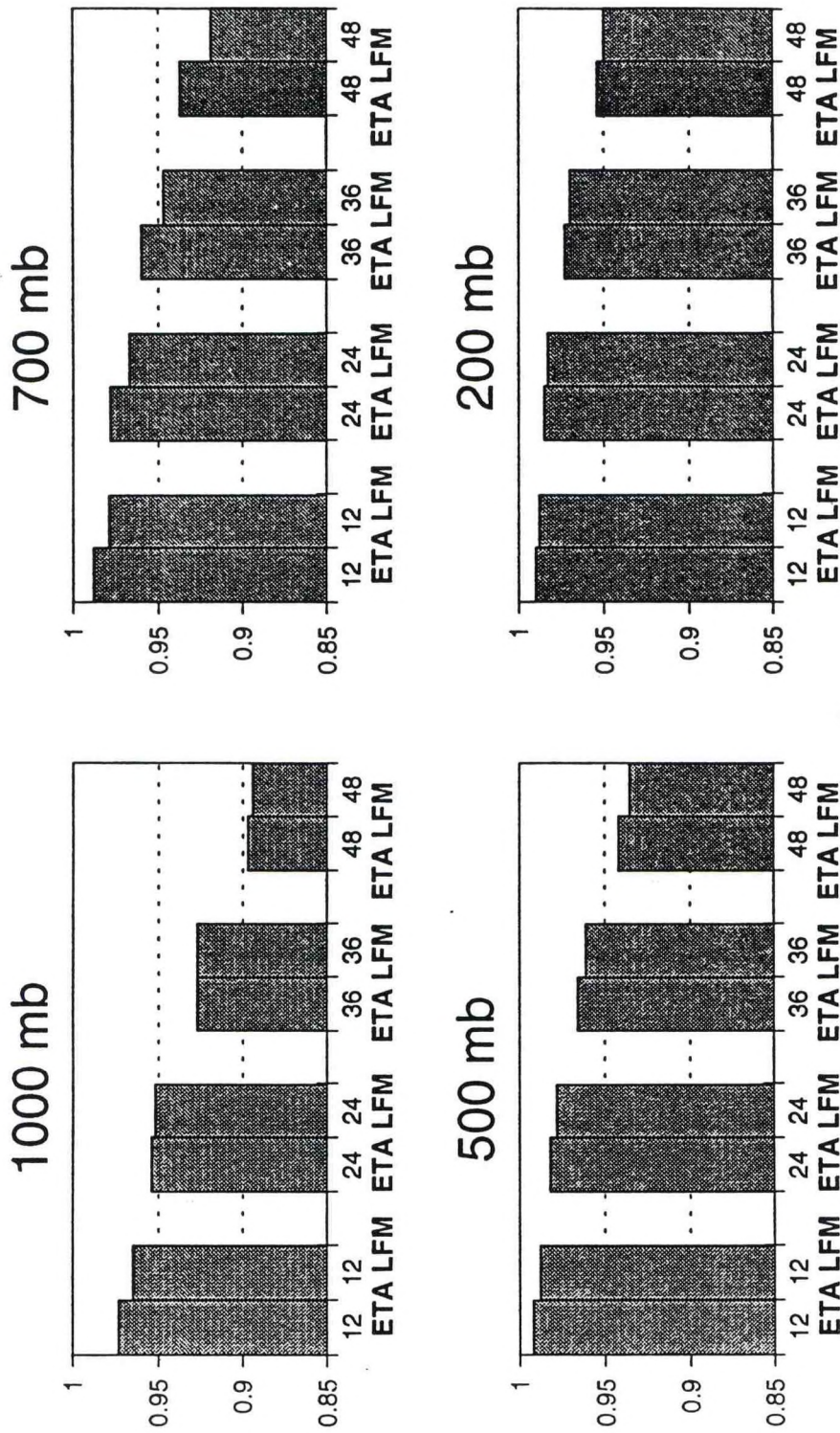
Figure 4. Anomaly correlation coefficient for height of indicated pressure surfaces for 12-, 24-, 36- and 48-hour forecasts (left to right) for the Eta model (left bar) and the LFM (right bar) computed over North American land points for the period March 2-31, 1993, using the RAFS analysis as truth.

TPB 412

Grid-Grid Verification - Rel. Humidity
North America 3/2/93 - 3/31/93

S1 Score 850 mb

Correlation Coefficient 850 mb

Tendency S1 Score 850 mb

Tendency Corr. Coef. 850 mb

Figure 5. Grid-to-grid (forecast versus analysis) verification scores for relative humidity at 850-mb level for 12-, 24-, 36- and 48-hour forecasts (left to right) for the Eta model (left bar) and the LFM (right bar); S1 score, correlation coefficient, tendency S1 score and tendency correlation coefficient (see text) computed over North American land points for the period March 2-31, 1993, using the RAFS analysis as truth.

Grid-Grid Verification - Rel. Humidity
North America 3/2/93 - 3/31/93

S1 Score 700 mb

Correlation Coefficient 700 mb

Tendency S1 Score 700 mb

Tendency Corr. Coef. 700 mb
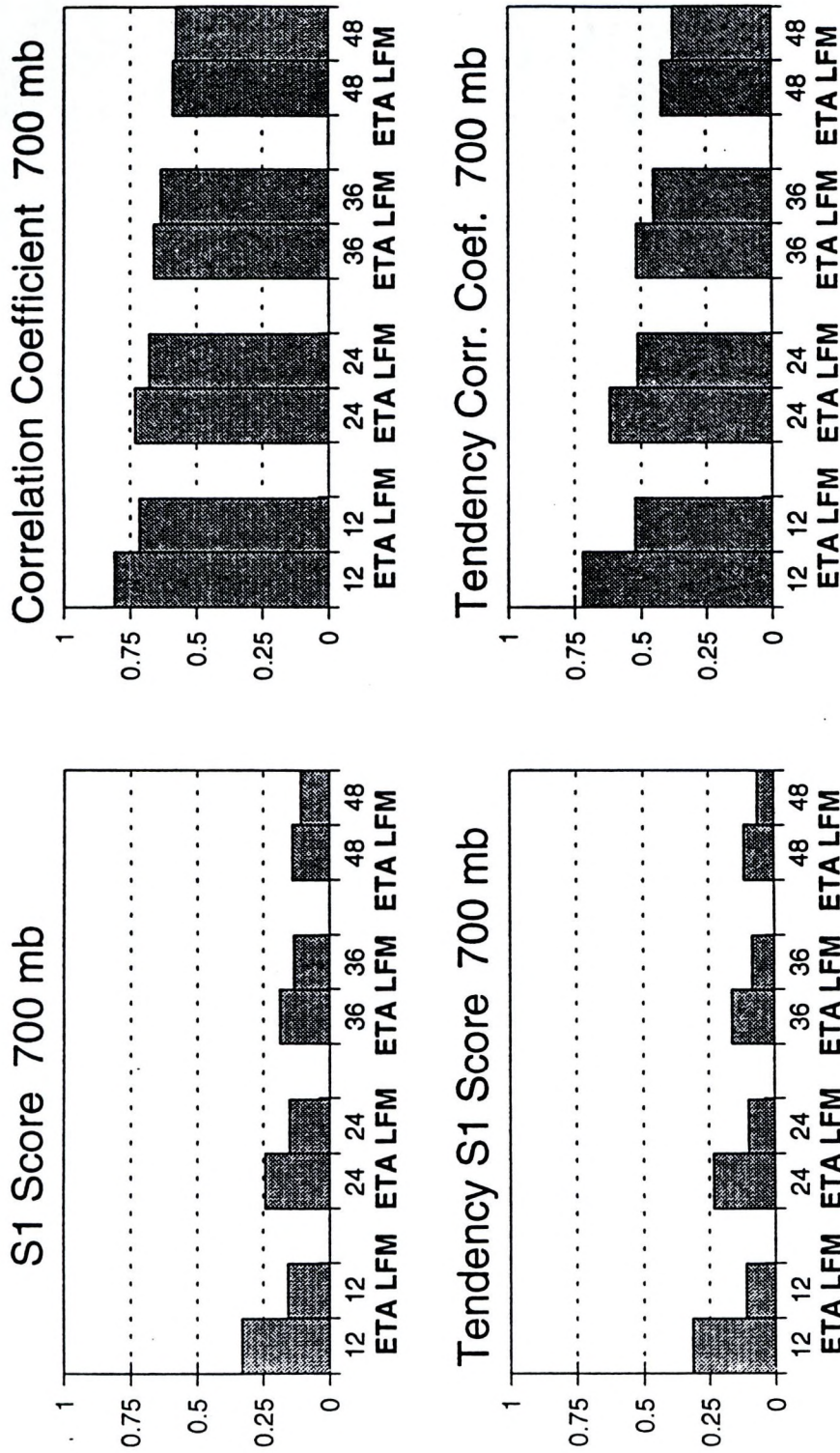
Figure 6. Grid-to-grid (forecast versus analysis) verification scores for relative humidity at 700-mb level for 12-, 24-, 36- and 48-hour forecasts (left to right) for the Eta model (left bar) and the LFM (right bar); S1 score, correlation coefficient, tendency S1 score and tendency correlation coefficient (see text) computed over North American land points for the period March 2-31, 1993, using the RAFS analysis as truth.

TPB 412

Verification Score Differences
ETA minus LFM
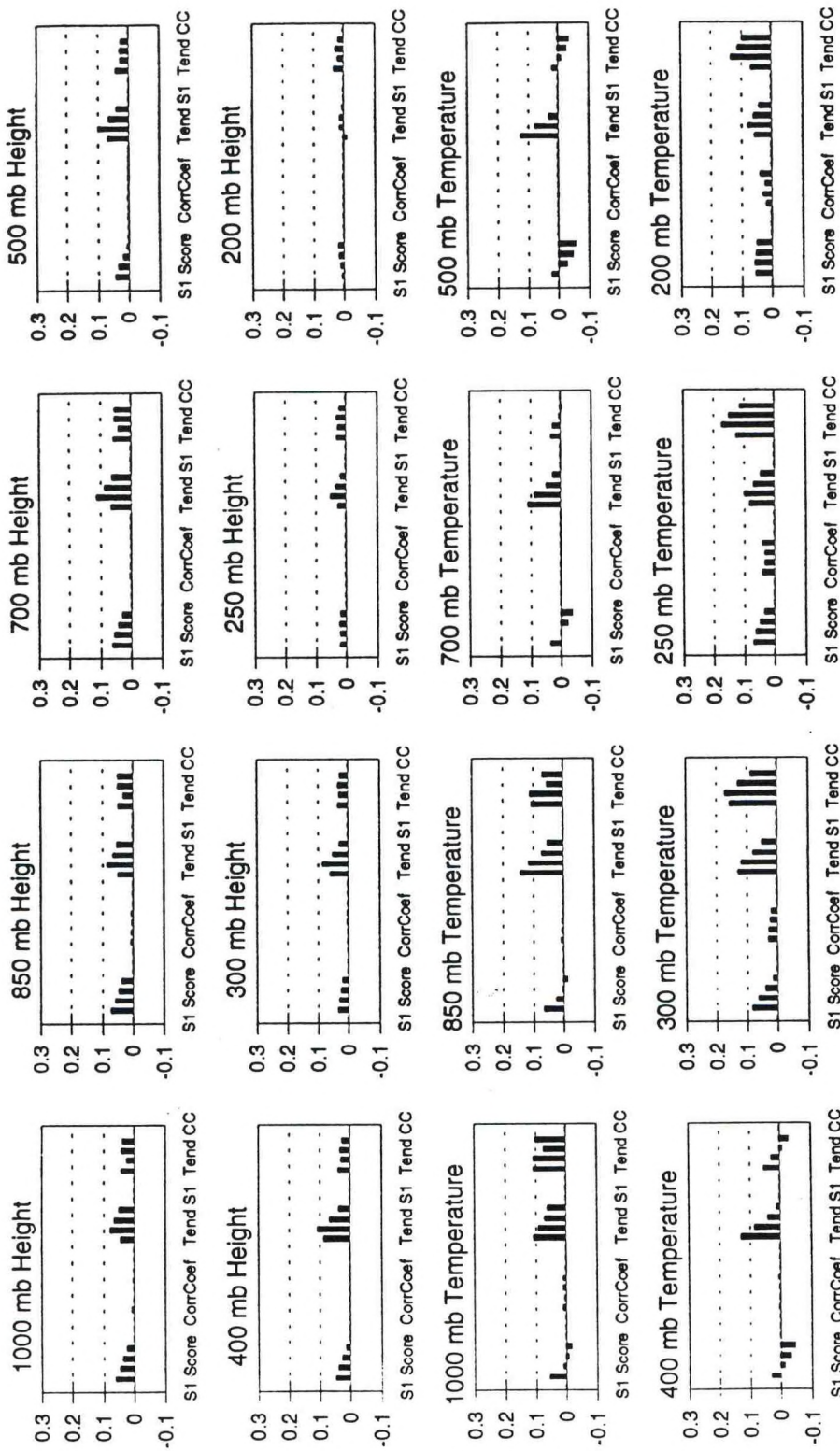
Figure 8a. Differences of the grid-to-grid verification scores (Eta score minus LFM score, see text) at each pressure level: the differences are plotted for 12-, 24-, 36- and 48-hour forecasts (left to right within each score); for S1 score, correlation coefficient, tendency S1 and tendency correlation coefficient (left to right within each variable); for height and temperature. Positive numbers indicate a better score for the Eta model vs. the LFM.
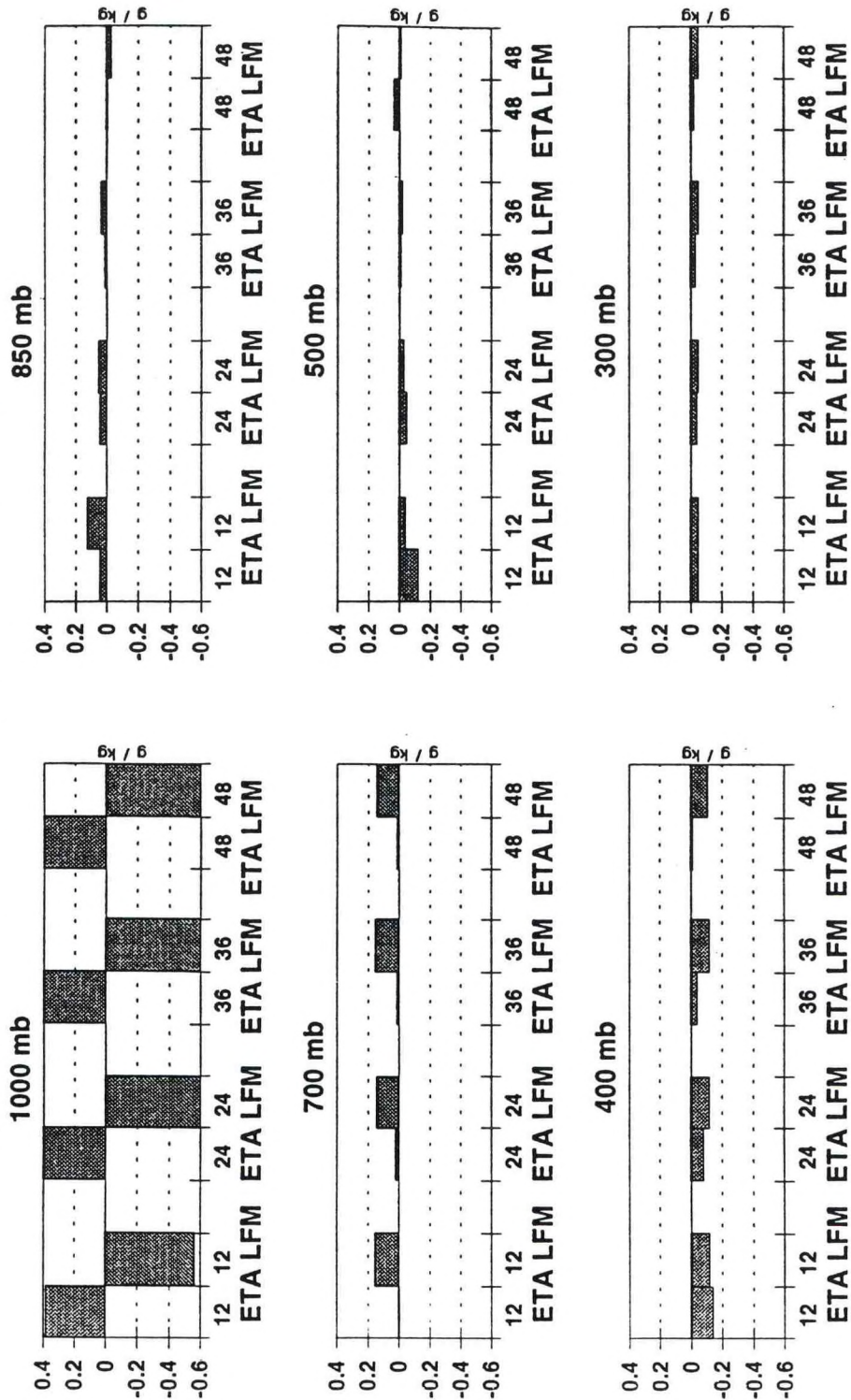
Figure 9. Bias (average Forecast minus Rawinsonde differences) for specific humidity (g/kg) at indicated pressure levels for 12-, 24-, 36- and 48-hour forecasts (left to right) for the Eta model (left bar) and the LFM (right bar) computed over North America for the period from February 26, 1993 to April 2, 1993. Positive values indicate the forecast is too wet.

Specific Humidity St.Dev Forecast-RAOB
North America 2/26/93 - 4/1/93
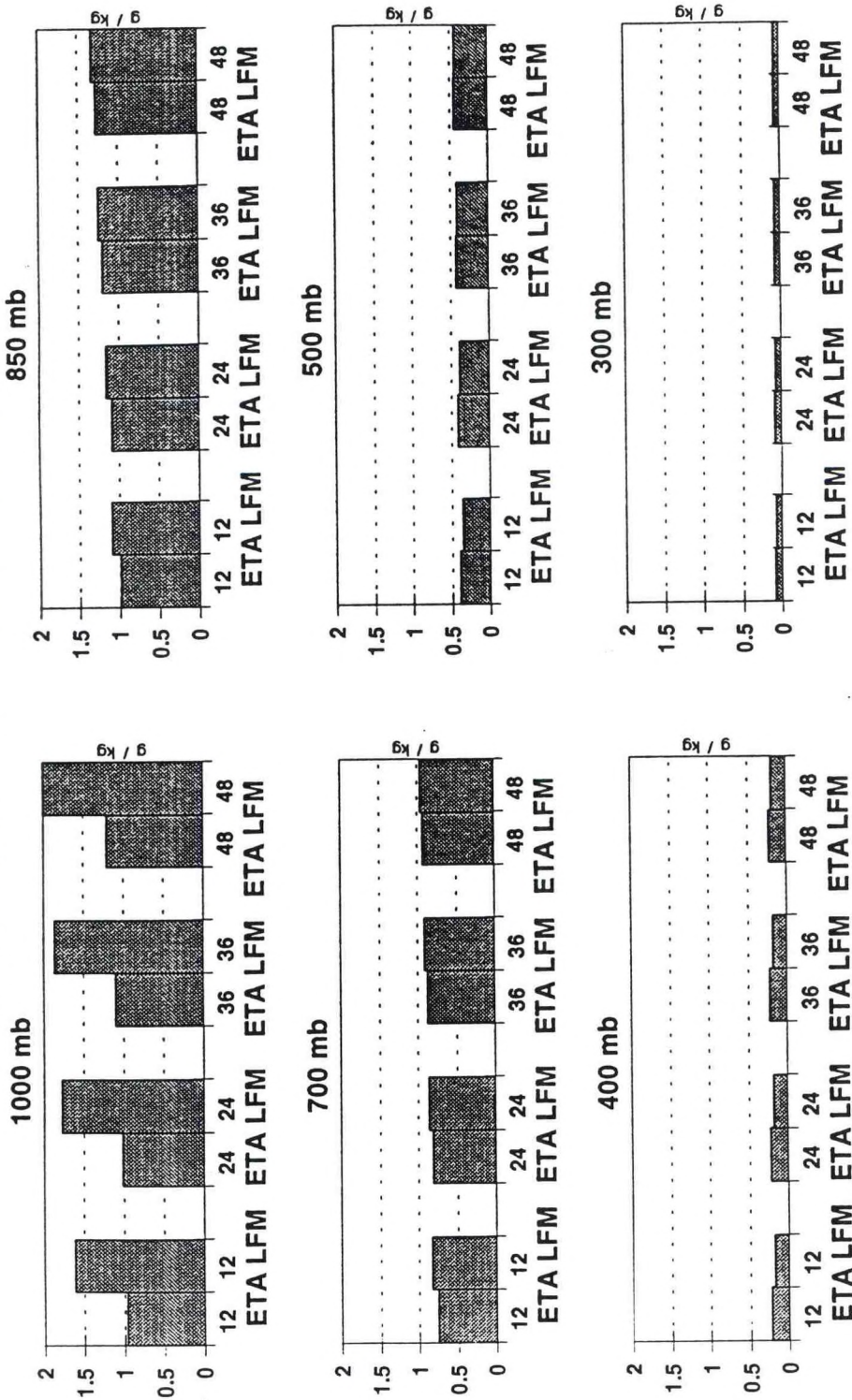
Figure 10. Standard deviation of Forecast minus Rawinsonde differences for specific humidity (g/kg) at indicated pressure levels for 12-, 24-, 36- and 48-hour forecasts (left to right) for the Eta model (left bar) and the LFM (right bar) computed over North America for the period from February 26, 1993 to April 2, 1993.

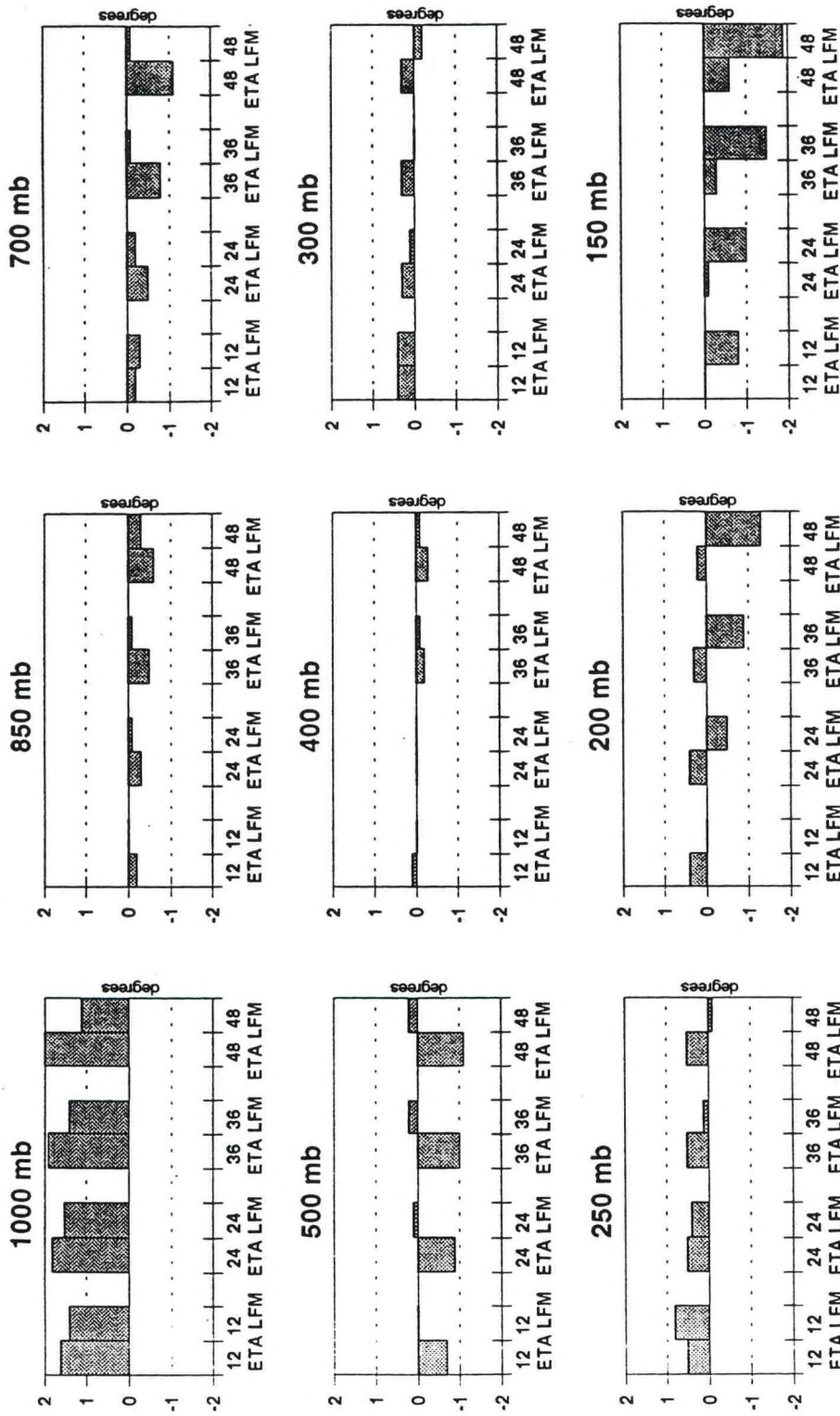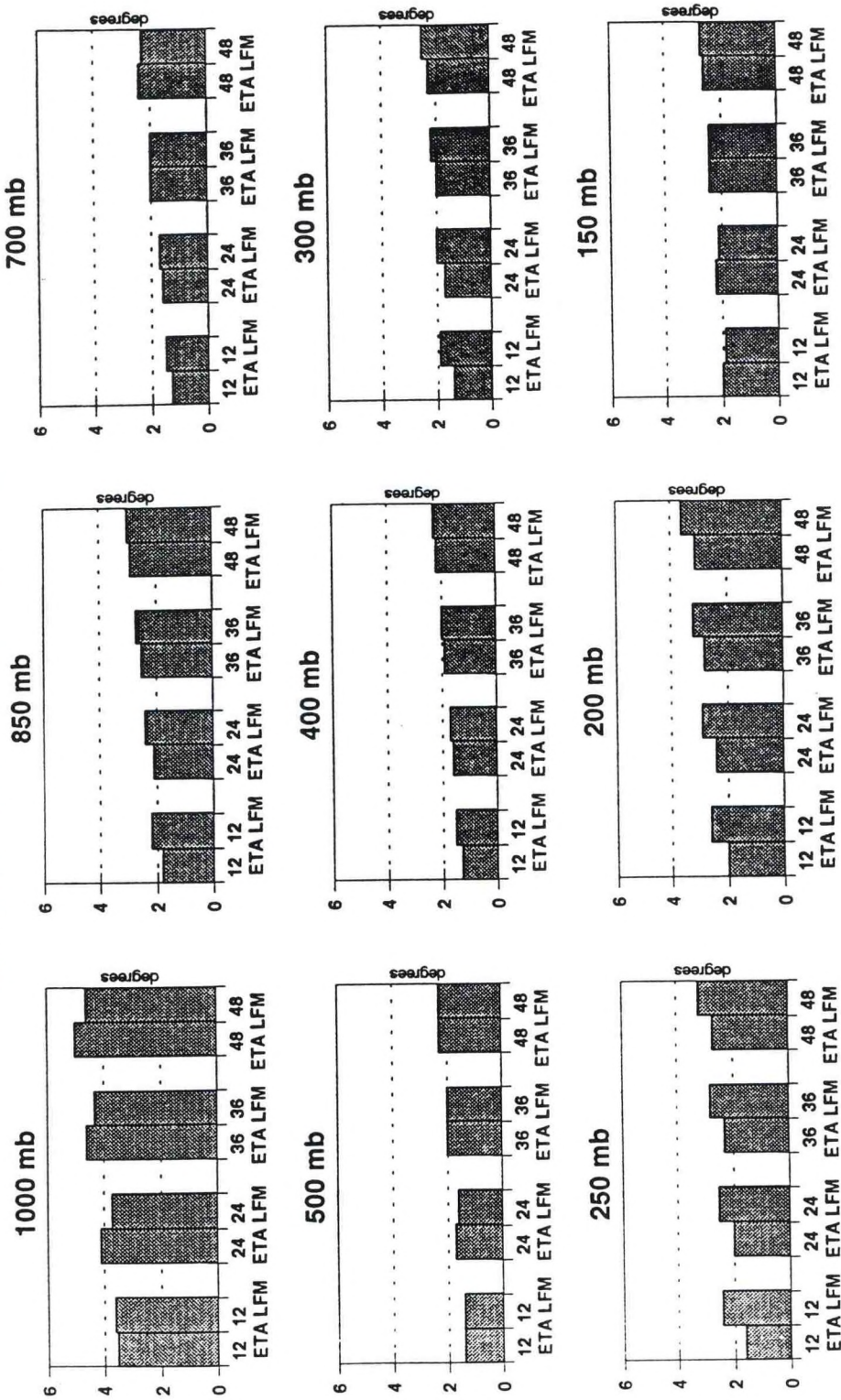# Height BIAS Forecast-RAOB
North America 2/26/93 - 4/1/93
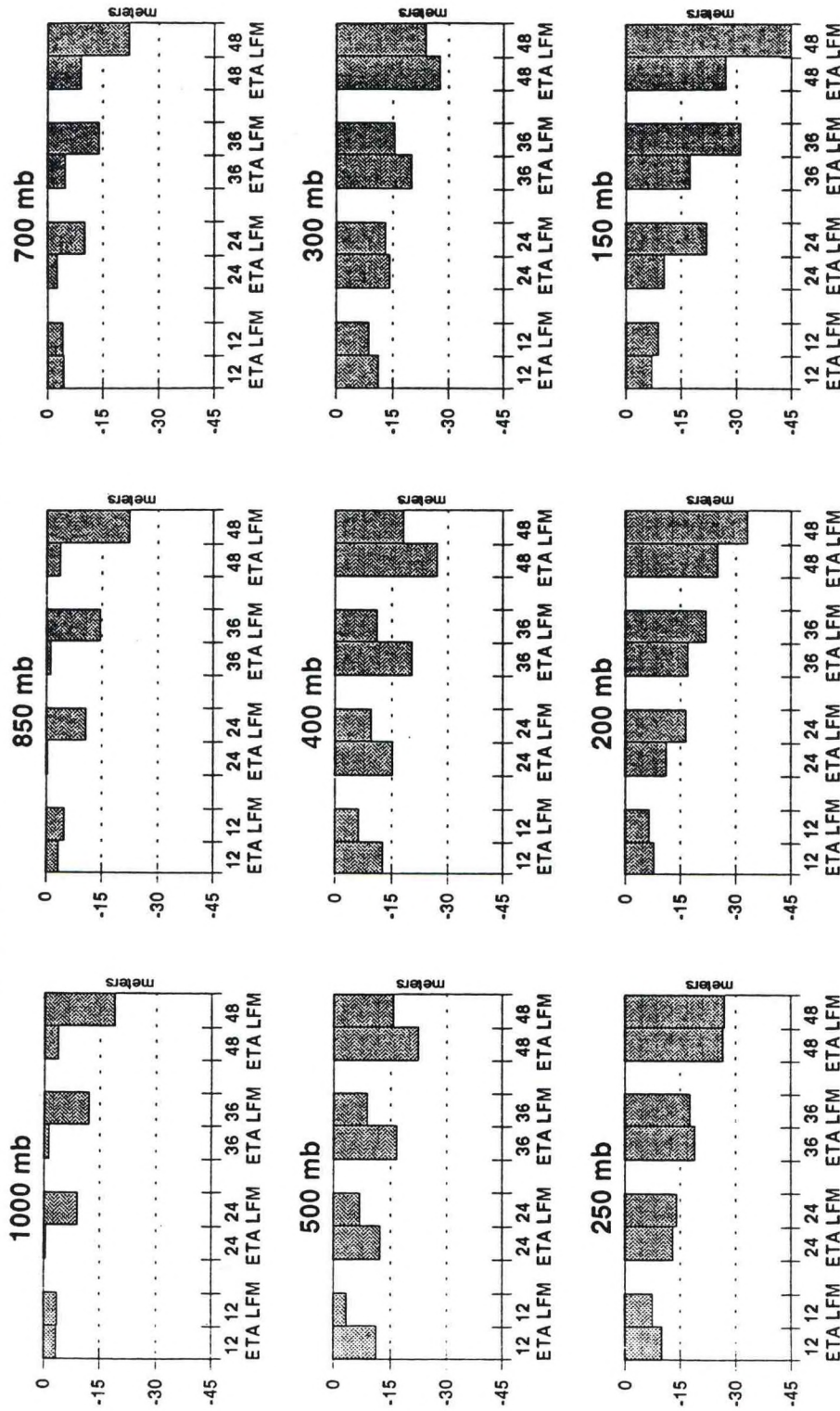
Figure 11. Bias (average Forecast minus Rawinsonde differences) for height (meters) of the indicated pressure surfaces for 12-, 24-, 36- and 48-hour forecasts (left to right) for the Eta model (left bar) and the LFM (right bar) computed over North America for the period from February 26, 1993 to April 2, 1993. Negative values indicate the forecast heights are too low.

Height St. Deviation Forecast-RAOB
North America 2/26/93 - 4/1/93
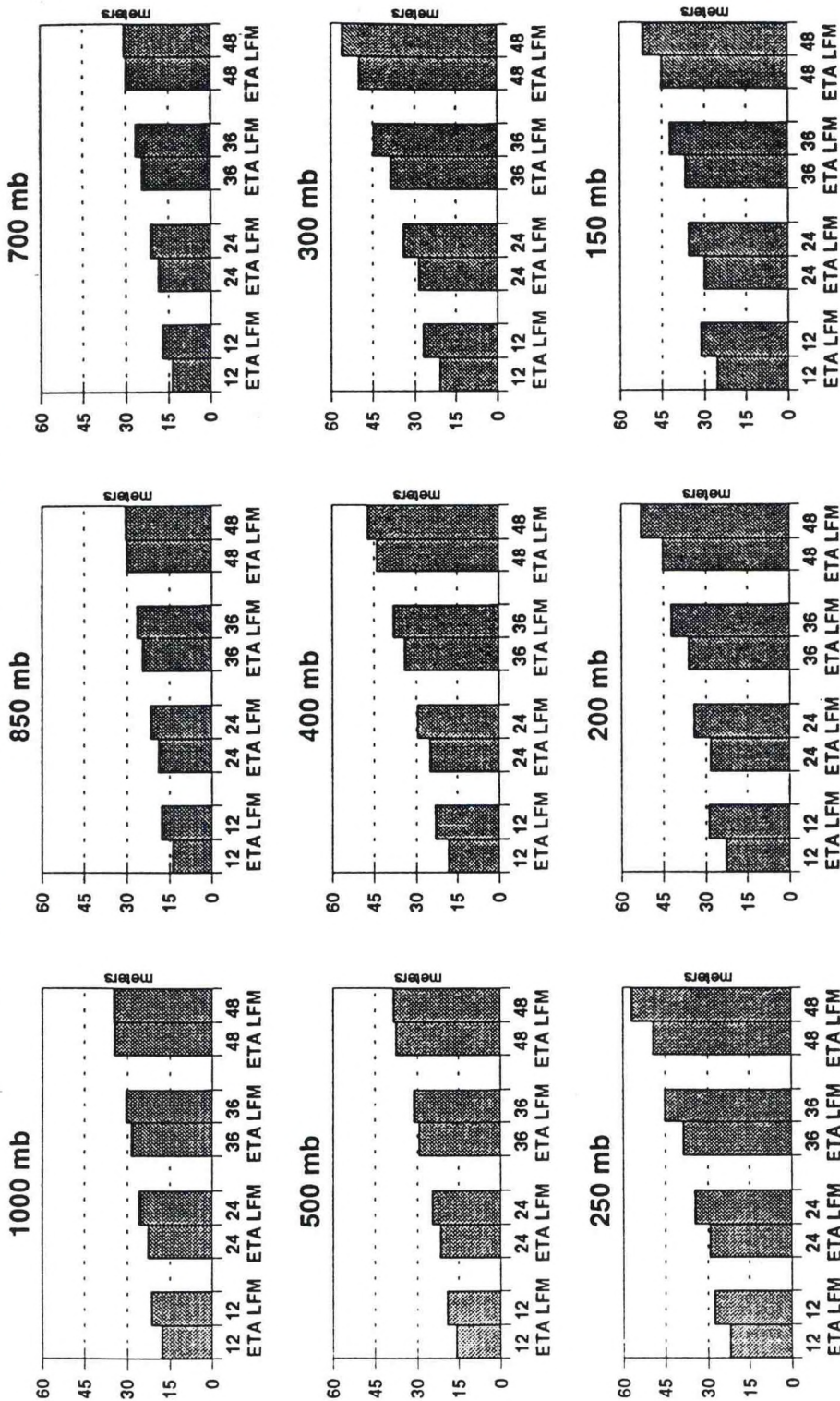
Figure 12. Standard deviation of Forecast minus Rawinsonde differences for height (meters) of the indicated pressure surfaces for 12-, 24-, 36- and 48-hour forecasts (left to right) for the Eta model (left bar) and the LFM (right bar) computed over North America for the period from February 26, 1993 to April 2, 1993.

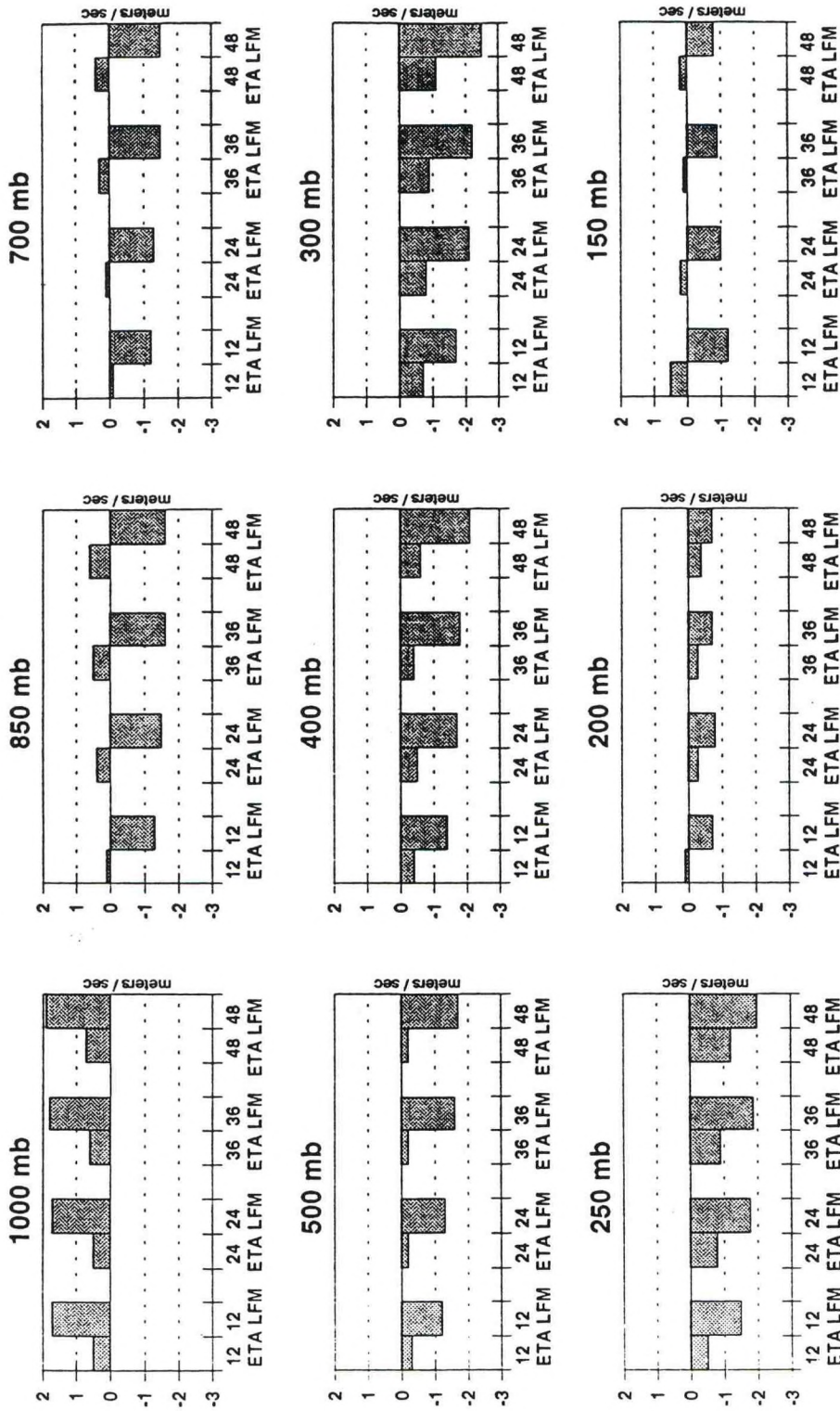# Temperature BIAS Forecast-RAOB
North America 2/26/93 - 4/1/93

Figure 13. Bias (average Forecast minus Rawinsonde differences) of temperature (°C) at the indicated pressure levels for 12-, 24-, 36- and 48-hour forecasts (left to right) for the Eta model (left bar) and the LFM (right bar) computed over North America for the period from February 26, 1993 to April 2, 1993. Negative values indicate the forecast is too cold.

Temperature St. Dev. Forecast-RAOB
North America 2/26/93 - 4/1/93

Figure 14. Standard deviation of Forecast minus Rawinsonde differences for temperature (°C) at the indicated pressure levels for 12-, 24-, 36- and 48-hour forecasts (left to right) for the Eta model (left bar) and the LFM (right bar) computed over North America for the period from February 26, 1993 to April 2, 1993.

24

Wind Speed BIAS Forecast-RAOB
North America 2/26/93 - 4/1/93

Figure 15. Bias (Forecast minus Rawinsonde differences) for wind speed (m/sec) at the indicated pressure levels for 12-, 24-, 36- and 48-hour forecasts (left to right) for the Eta model (left bar) and the LFM (right bar) computed over North America for the period from February 26, 1993 to April 2, 1993. Negative values indicate forecast winds are too weak.
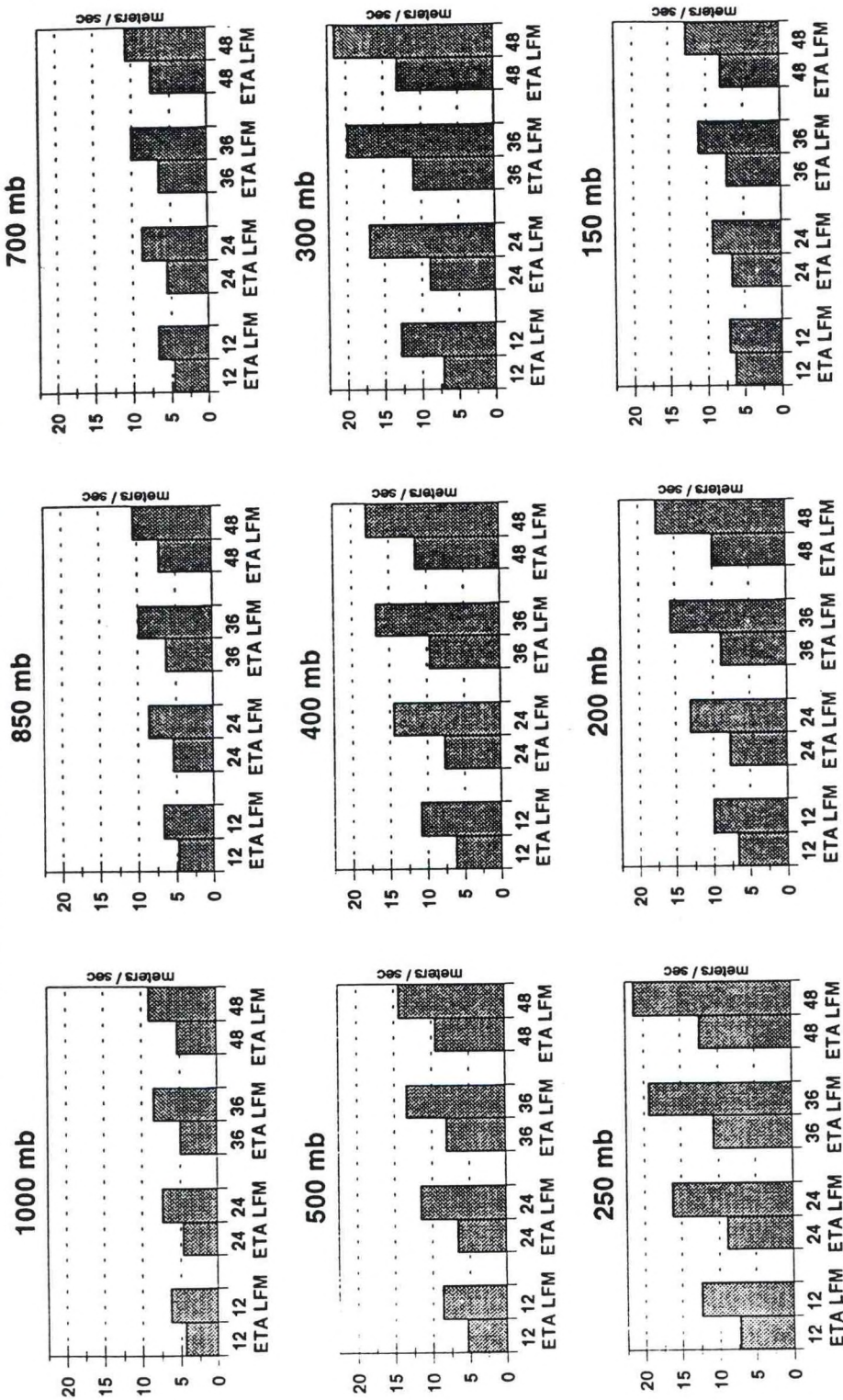
Figure 16. Root-mean-square of Forecast minus Rawinsonde differences in the vector wind (m/sec) at the indicated pressure levels for 12-, 24-, 36- and 48-hour forecasts (left to right) for the Eta model (left bar) and the LFM (right bar) computed over North America for the period from February 26, 1993 to April 2, 1993.
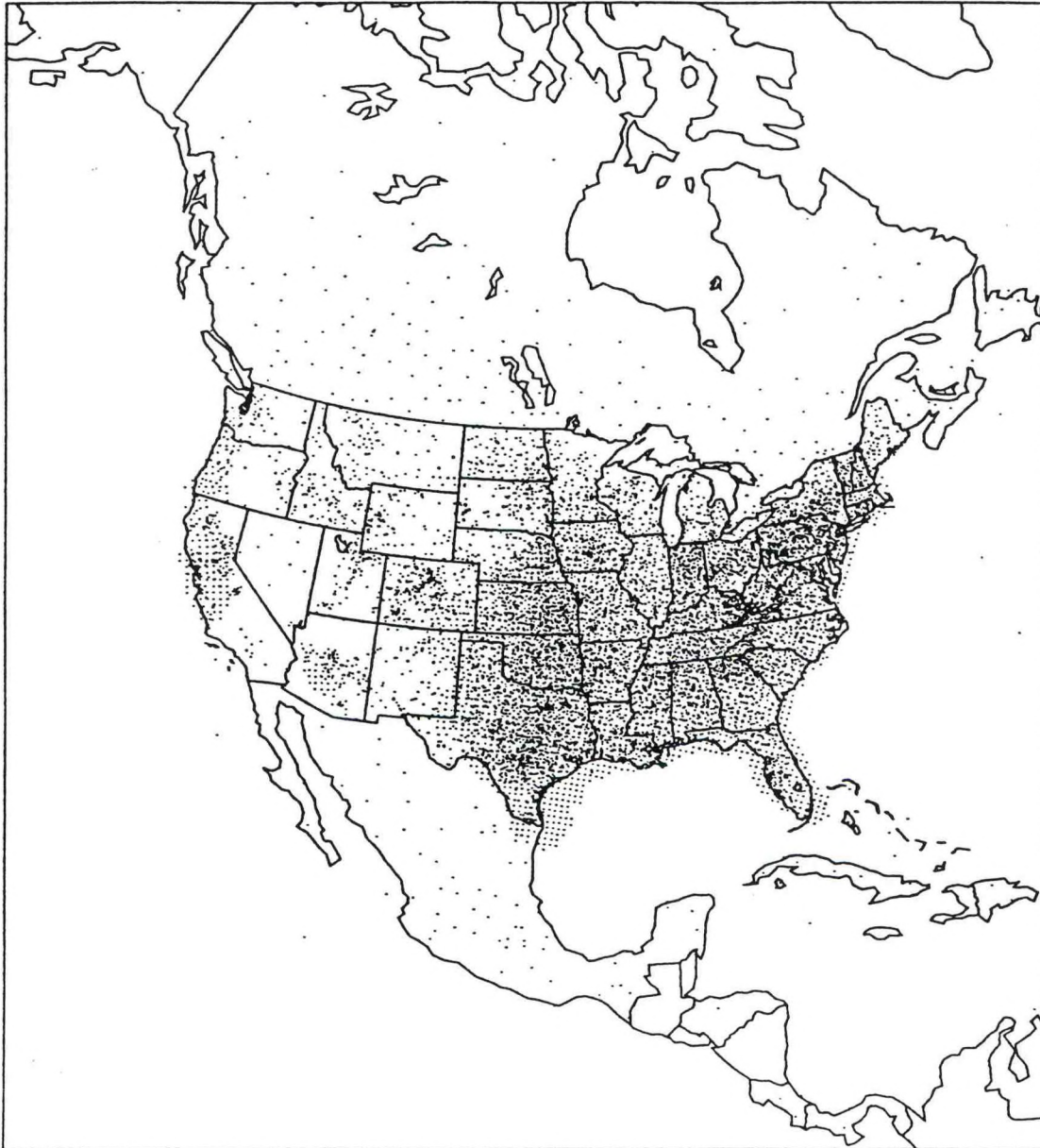
Figure 17. Locations of stations reporting 24-hour precipitation amounts between June 1991 and February 1992. Note: station locations off the coasts are derived from manually-digitized radar (MDR) and are not considered.
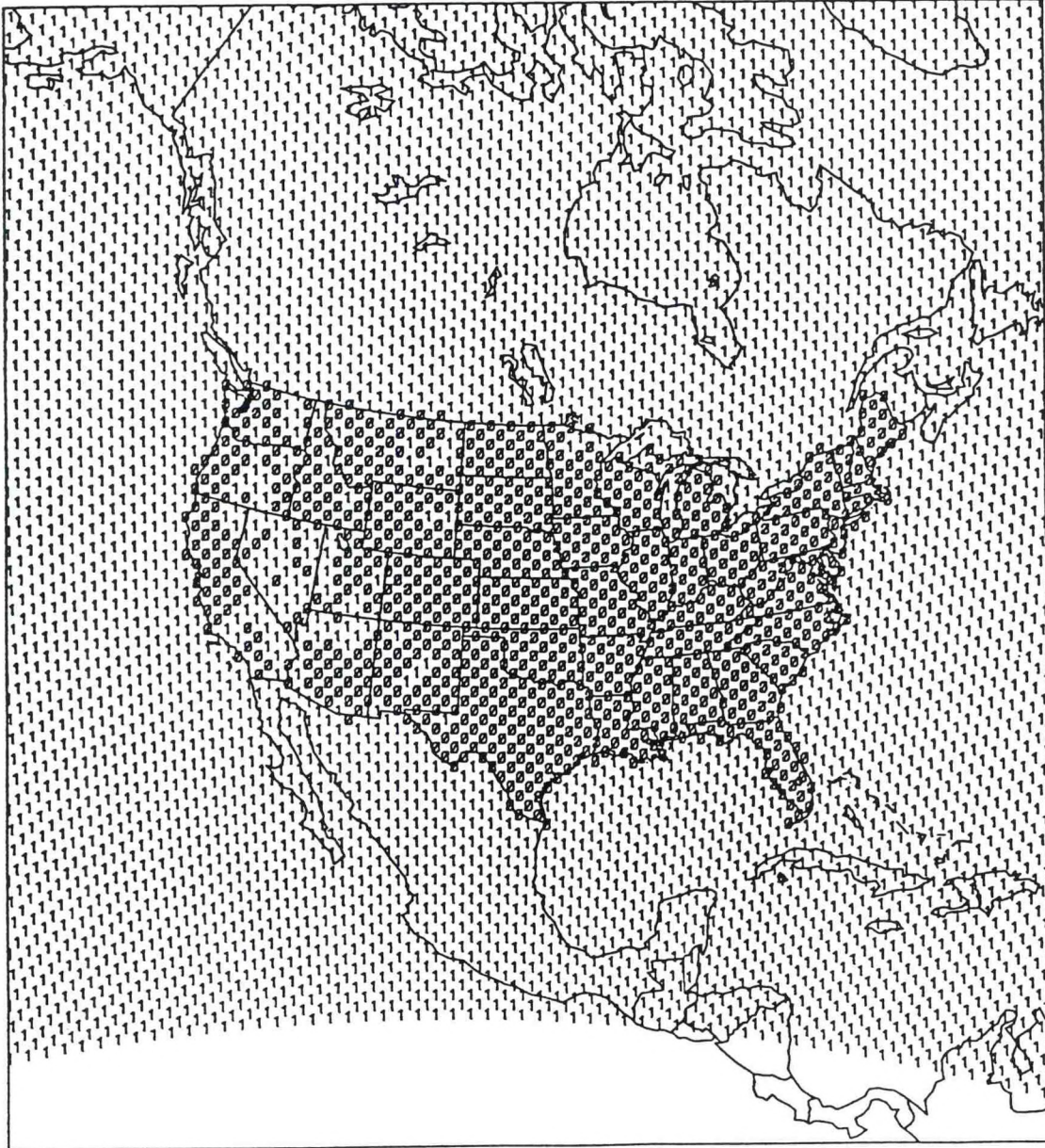
Figure 18. Eta Model grid locations at which precipitation verification was performed (1001 points over continental United States, marked as 0's). The remaining points, where verification was not performed, are marked with 1's.
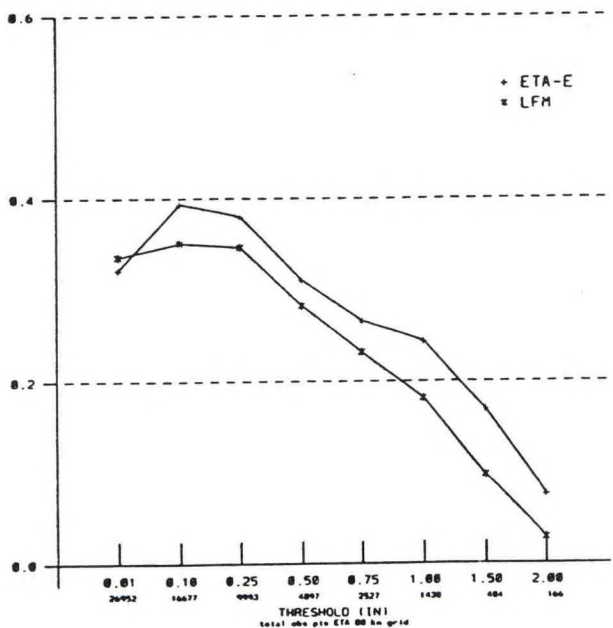
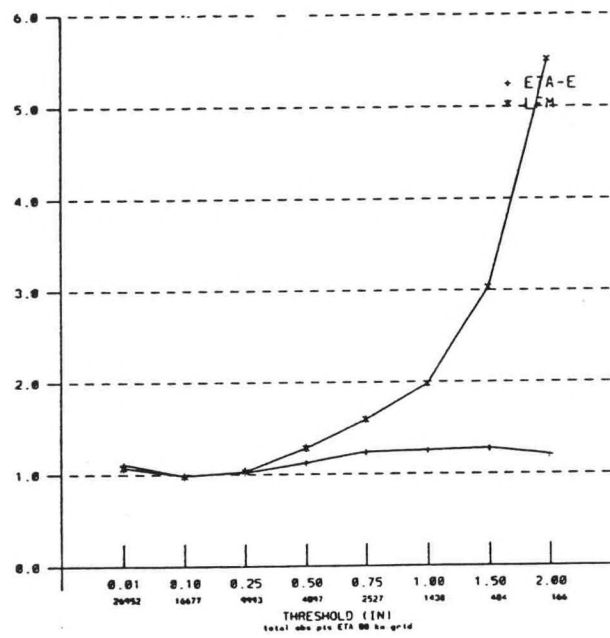**Figure 21.** Same as Figure 19, except for the period April 1-24, 1993.

Figure 22. Same as Figure 20, except for the period April 1-24, 1993.
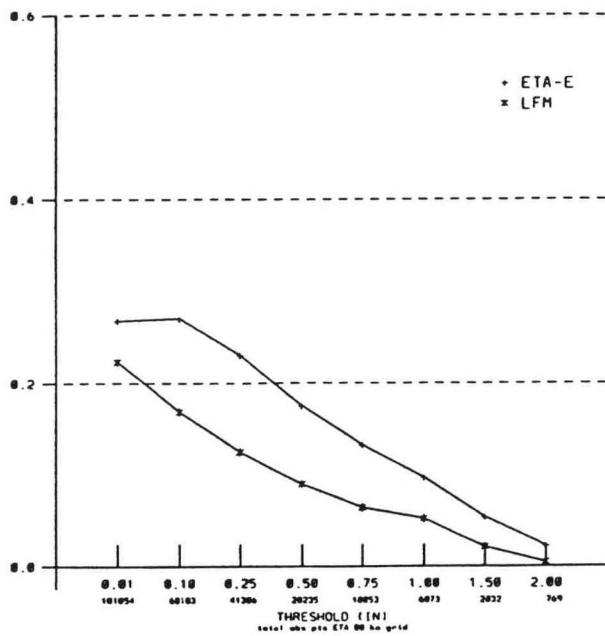
Figure 23. Same as Figure 19, except for the period June 1 - August 31, 1992.
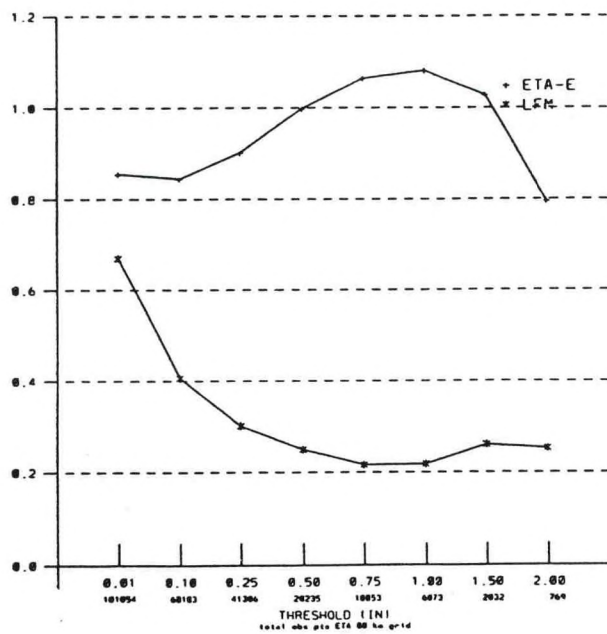

Figure 24. Same as Figure 20, except for the period June 1 - August 31, 1992.